An Observing System Simulation Experiment (OSSE) for the Aquarius/SAC-D soil moisture product

Cintia A. Bruscantini, *Student Member, IEEE,* Wade T. Crow, Francisco Grings, Pablo Perna, Martin Maas and Haydee Karszenbaum.

Abstract

An Observing System Simulation Experiment for the Aquarius/SAC-D mission has been developed for assessing the accuracy of soil moisture retrievals from passive L-band remote sensing. The implementation of the OSSE is based on: a 1-km land surface model over the Red-Arkansas River Basin, a forward microwave emission model to simulate the radiometer observations, a realistic orbital and sensor model to resample the measurements mimicking Aquarius operation, and an inverse soil moisture retrieval model. The simulation implements a zero-order radiative transfer model. Retrieval is done by direct inversion of the forward model. The Aquarius OSSE attempts to capture the influence of different error sources: land surface heterogeneity, instrument noise and retrieval ancillary parameter uncertainty on the accuracy of Aquarius surface soil moisture retrievals. In order to assess the impact of these error sources on the estimated volumetric soil moisture, a quantitative error analysis is performed via the comparison of footprint-scale synthetic soil moisture with 'true' soil moisture fields obtained from the direct aggregation of the original 1-km soil moisture field fed into the forward model. Results show that, in heavily vegetated areas, soil moisture retrievals present a positive bias that can be suppressed with an alternative aggregation strategy for ancillary parameter vegetation water content (VWC). Retrieval accuracy was also evaluated when adding errors on 1-km VWC (which are intended to account for errors in VWC derived from remote sensing data). For soil moisture retrieval RMSE of the order of 0.05%vol/vol, relative error bias on VWC should be less than 12%.

Index Terms

Aquarius; Observing System Simulation Experiment; soil moisture.

C. Bruscantini, F. Grings, P. Perna, and H. Karszenbaum are with the Instituto de Astronomía y Física del Espacio (IAFE), Argentina (e-mail: cintiab@iafe.uba.ar).

W. Crow is with the Hydrology and Remote Sensing Laboratory, USDA-ARS Beltsville, USA

J. Jacobo-Berlles is with the Departamento de Computación, Facultad de Ciencias Exactas y Naturales (FCEN), Universidad de Buenos Aires (UBA), Argentina.

I. Introduction

An Observing System Simulation Experiment (OSSE) is a simulation designed to mimic as closely as possible a given satellite mission, in order to study one or several characteristics of its operation. In general, OSSEs are developed to study final product characteristics as a function of system characteristics. In the past, OSSEs have been carried out to study the impact of land surface heterogeneity [1], instrument error and parameter uncertainty on soil moisture products [2] for the AMSR-E and Hydros missions. In these studies it was shown that OSSEs are a useful tool to analyze the error budget of a given sensor from a system theory point of view, in order to identify areas where the error is large and can be reduced by relatively inexpensive means.

In this paper, a similar analysis is performed using an OSSE developed for the Aquarius/SAC-D mission. The mission is a collaboration between NASA and the Space Agency of Argentina (Comisión Nacional de Actividades Espaciales). Aquarius main scientific objective is to provide global measurements of sea surface salinity. Therefore, some simulation work have been developed to study sea surface salinity product [3]. However, measurements of the L-band radiometer on board the satellite are also capable to generate soil moisture global maps.

Unlike previous OSSE works cited, the OSSE described here incorporates Aquarius unique sensor characteristics (e.g. antenna footprints, radiometer measurement procedure, soil moisture composite) and a detailed error analysis on ancillary parameter VWC.

This OSSE includes four elements: 1) a land surface model (LSM) to generate 1-km resolution geophysical data fields; 2) a microwave emission model (MEM) to simulate soil surface brightness temperature (Tb) from soil properties at 1 km; 3) a system and orbital model (SOM) to simulate Aquarius measurements at 100 km (which includes instrument and acquisitions strategy artifacts); and 4) a retrieval model (RM) to estimate soil moisture from Aquarius measurements at 100 km and aggregated ancillary data.

Fig. 1 illustrates the key components included in the observing system simulation experiment and the data flow.

Generally speaking, there are four different types of errors captured by the OSSE:

1) **Heterogeneity effects** - sampling and nonlinearity effects associated with land surface heterogeneity and running the retrieval model at a coarser spatial resolution than forward model. These errors include the impact of non linearities in the MEM and RM and gridding effects associated with the gain function.

2) **Observation noise effects** - errors that arise when adding synthetic noise to the footprint-scale Tb. These errors correspond to system measurement errors.

3) **Retrieval parameter error effects** - errors that arise when adding synthetic noise to the footprint-average retrieval parameters. These errors are related to uncertainties on the ancillary parameters needed in the RM.

4) **Forward/retrieval model incompatibilities** - errors that arise when the retrieval model is structurally inadequate [4].

Of course, real retrievals are degraded by all four effects. Nevertheless, using OSSEs outputs it is possible to isolate the impact of all four error sources. Here, we focus on OSSE simulations corresponding to land surface heterogeneity effects (1), observation noise effects (2) and retrieval parameter error effects (3). Simulations are presented for all the cases, and a description of how errors evolve from case-to-case is also offered.

II. Methodology

A. Land Surface Model

High resolution geophysical variables used as the reference 'true' fields needed for the simulation were generated via a land surface model (LSM) at 1-km spatial resolution within $250,000 km^2$ Red-Arkansas River Basin (south-central US) for 4 months in summer of 1994. The static dataset used for the nature run include a land cover and soil texture database, a digital elevation model and a NDVI database, all at 1 km resolution. The LSM used for the simulations is the TOPLATS hydrological model [5]. The three LSM predictions are: 0 to 5 cm integrated surface soil moisture in volumetric (m^3/m^3) units, surface 'skin' temperature and 5-cm soil temperature. Outputs were generated at 6 p.m. local time in the Central US, corresponding to Aquarius ascending overpass time. Therefore, only ascending results were simulated and analyzed.

B. Microwave Emission Model

Radiometer observations were simulated at Aquarius frequencies (1.413 GHz), polarization (h and v) and incidence angles (28.7°, 37.8°and 45.6°for inner, middle and outer beam) at 1 km spatial resolution. Radiometer brightness temperature was computed based on a zero-order radiative transfer model that

includes vegetation and soil components as [6]

$$\begin{aligned} Tb_p =& Ts(1-r_p)exp\left(-\frac{\tau}{cos\theta}\right) + Tc(1-\omega) \\ & \times \left(1-exp\left(-\frac{\tau}{cos\theta}\right)\right)\left(1+r_p exp\left(-\frac{\tau}{cos\theta}\right)\right) \end{aligned} \quad (1)$$

where *p* refers to polarization, *Ts* is 5-cm soil temperature and *Tc* is surface skin temperature (both derived from the LSM), r_p is the soil reflectivity, θ is the look angle, τ is the nadir vegetation opacity, ω is the vegetation single scattering albedo. Vegetation opacity is assumed to be unpolarized and is defined as $\tau = b\,VWC$, where b is a land cover depending coefficient and VWC is vegetation water content (kg/m^2).

The surface roughness effect over the modeled brightness temperature was approximated as $r_p = r_{sp}exp(-h)$ where h is related to the root mean square surface height and r_{sp} is the reflectivity of the equivalent smooth soil surface. Values for these land cover depending ancillary parameters were obtained from [1].

Finally, dielectric constant is obtained from soil moisture and soil type using semiempirical dielectric mixing model proposed by Dobson et al. [7].

High resolution inland water pixels were not considered for the analysis.

C. Sensor and Orbital Model

The SOM is based on a Matlab routine that implements SGP4 orbit propagation. Aquarius orbital parameters considered in the SOM were: 98.0126 degree inclination, 0.0012 eccentricity, 18:00 mean local mean time of ascending node, 7028.871 km mean semi-major axis, 90 degree mean argument of perigee and 657 km satellite height.

The synthetic 1-km Tb are weighted by a $sinc^2$ function, a theoretical approximation of the Aquarius antenna patterns with matching -3 dB footprints. The ground projected axis of the footprints are: 74 km along track x 94 km cross track for the inner beam, 84x120 km for the middle beam and 96x156 km for the outer beam yielding a total cross track of 390 km [8]. For each of the three beams, 1 km resolution gain patterns were projected on the ground as in [9]. Patterns were rotated and located to move along with the satellite motion. Geolocation of observations was associated to the latitude and longitude of the center of the footprint. Spatially independent Gaussian noise with standard deviation of $1\,K$ for brightness temperature was added to measurements at this stage when accounting for radiometer instrumental noise

effect. The chosen measurement error is high considering the 0.38 K error expected per observation described in [10]. Observations were then averaged to a time step of $1.44\,s$ (i.e. 12 Tb samples), to match the temporal resolution of Aquarius Level 2 [11] and Aquarius measurement procedure [8].

D. Retrieval Model

The OSSE implements the single channel retrieval algorithm (SCA) [12] to estimate soil moisture from simulated brightness temperature. This is accomplished by directly inverting the implemented forward model. Soil moisture was achieved from reflectivity coefficient via Fresnel equations and the dielectric mixing model used in MEM. Auxiliary data for estimating soil moisture are the ancillary parameters at footprint scale. These values are derived by linear averaging 1-km emission parameters used as inputs to the simulation.

In previous studies [13], it was shown that the most critical value in terms of soil moisture retrieval errors is the VWC. To evaluate the effect of subfootprint-scale land surface heterogeneity, two methods of aggregating VWC were evaluated. Linear averaging (AVE) of 1-km VWC and an alternative aggregation scheme (AGG) for VWC, derived from theoretical considerations (see [14]), resulting as follows

$$VWC_{agg} = \left[ln\left(\sum_{i=1}^{n} A^{VWC_i} \right) - ln(n) \right] / ln(A) \tag{2}$$

where $A = exp(-2b/cos\theta)$, with θ Aquarius incident angle and b the vegetation parameter that relate vegetation opacity to VWC. Uncertainties in ancillary parameters were accounted for by adding noise to some footprint-resolution parameters in some OSSE's runs. Gaussian noise with zero mean and standard deviation of: 1 K for Ts and Tc, 1% relative error for sand, clay and VWC, and 0.005 for b and h (cm).

E. Composite

To mimic Aquarius Level 3 processing, retrieved soil moisture at center of footprints location for the three beams were mapped onto a fixed weekly soil moisture product of 1° grid. Composite pixels may arise from observations of different beams and the resulting image will be the standard Aquarius soil moisture product. In order to generate the composite, three sampling methods were implemented: (1) nearest neighbour (NN), (2) a weighing function (WF) and (3) local quadratic polynomial fitting (LP) with bandwidth 100 km [15]. In (2), each pixel value depends upon the spatial location of each observation (distance from the sample to the center of the pixel, $distance$) as well as the soil moisture

value ($sample\,value$) as follows,

$$Pixel\,value = \frac{\sum_{i=1}^{n} sample\,value_i/distance_i}{\sum_{i=1}^{n} 1/distance_i} \tag{3}$$

Image pixel values derived for interpolation (1) and (2) were obtained binning soil moisture Level 2 product onto a 1° grid (Fig. 2).

III. Results

Soil moisture runs from April 2^{nd} to July 30^{th}, 1994 were used in this analysis. Since Aquarius has a 7 days repeat pass, 17 weekly product images were obtained. Each 7-day retrieved soil moisture image was obtained through composing observations from 7 different days.

A. Total Error Analysis

OSSE's soil moisture was retrieved with the SCA for the two polarization channels, the three different Aquarius beams, the two VWC aggregation strategies and the three different soil moisture composites. For every run alternative, three outputs were obtained: (1) no noise case, (2) Tb with Gaussian noise case (observation noise effects in Section II-C) and (3) Tb and ancillary parameters with Gaussian noise case (observation noise and retrieval parameter error effects in Section II-D). For assessing the impact of these different error sources and be able to quantify their influence over the final product (weekly soil moisture), two error metrics were taken into consideration. For every output, correlation (ρ) between synthetic soil moisture (sm_0) and weekly-averaged 'true' soil moisture degraded at coarse resolution (sm_g), as well as root mean square error, RMSE, were computed.

$$RMSE = \sqrt{\frac{1}{n}\sum_{i=1}^{n}(sm_0 - sm_g)^2} \tag{4}$$

In Table I the error metrics for each case are displayed. The simulation were run for three composite methods (NN, WF and LP), the two VWC aggregation methods (AVE and AGG), and three noise cases (no noise (nn), instrumental noise (i) and instrumental noise and ancillary parameters uncertainties (i+p)). In all the tested cases, estimation using the vertical polarization channel displays slightly higher estimation accuracy than retrieval from horizontal channel. This result is controversial, since it does not agree with field experiments nor theoretical results, which predicts a higher sensitivity of the H channel. In general, SCA uses horizontal polarization to retrieve soil moisture because of its higher dynamic range on Tb.

Moreover, horizontal channel is expected to have better performance since calibration bias of the Aquarius radiometer is higher for the vertical polarization [16]. However, vertical polarization was also pinpointed as the best channel option for SCA in [17] where it was established that this channel is least sensitive to variable surface roughness and vegetation canopy.

With regards to VWC aggregation, applying alternative aggregation method proposed in [14] results in an improvement on the estimation in all cases, as expected. Finally, the errors associated with composite strategy were evaluated. The estimation performance slightly improves when using the weighing function composite. Furthermore, this interpolation exhibits less sensitivity to instrumental noise and parameter uncertainties.

Total error as a function of beam number was also evaluated. Differences on retrieval performance between beams is expected since the three Aquarius beams have different incidence angle and footprint dimensions. Since error analysis is performed after composing, beam performance differentiation cannot be directly assessed. Though, simulations for Level 2 product showed that middle beam exhibits the highest accuracy and the outer beam the lowest. As an example, in the case where neither instrumental noise nor ancillary parameter uncertainties are added and alternative aggregation of VWC is applied, inner beam has ρ_h=0.969, $RMSE_h$=0.023, ρ_v=0.976 and $RMSE_v$=0.020, middle beam ρ_h=0.984, $RMSE_h$=0.017, ρ_v=0.986 and $RMSE_v$=0.016 and the outer beam ρ_h=0.959, $RMSE_h$=0.027, ρ_v=0.960 and $RMSE_v$=0.027. Nevertheless, since the composite is constructed using all the three beams, these effects are not relevant to the L3 product.

B. Parameter VWC

1) VWC Aggregation: Resolution degradation of VWC was obtained through two different aggregation approaches: AVE and AGG (see Eq. (2)) over high resolution VWC to degrade to final product spatial resolution. An error analysis was performed to derive the accuracy of synthetic soil moisture retrieved with both schemes (Fig. 3(a) and 3(b)). Results suggest that linear aggregation of vegetation water content produced overestimation of soil moisture for heavily vegetated surfaces. The alternative aggregation strategy gives rise to lower VWC, which turns over lower retrieved soil moisture. Therefore, this method resulted on an improvement on soil moisture estimation accuracy.

To understand the errors that arise from the two different approaches, comparison between aggregated and averaged VWC against the corresponding effective VWC values was performed following the methodology in [14] over the 17 weeks simulation period. Effective VWC values are defined as the

ones that minimize RMSE in soil moisture retrievals for a given condition. Results are illustrated in Fig. 4 (the value of the b parameters needed for the alternative aggregation approach was obtained through linear average of high resolution b). As seen, aggregated VWC presents better agreement with effective VWC. These results agree with the outputs obtained from the OSSE: averaged VWC displays a positive bias in VWC which increases as vegetation becomes denser and produce a positive bias in estimated soil moisture. On the contrary, retrieved soil moisture with the alternative aggregation approach shows a better agreement with ground soil moisture.

An important feature that is observed in Fig. 4 is an horizontal stripes pattern. This artifact is produced because, for a given pixel, VWC and b parameters remain constant over the simulation period but the effective VWC changes through time. Effective VWC changes imply that the VWC value which will lead to the minimum error in soil moisture estimation changes over time. This change should be related to the variables that change over time in the OSSE, which are: soil moisture, soil temperature and canopy temperature. Thus, the change in the effective VWC value is presumably related to the aggregation method of these parameters. Although these errors are small compared with VWC ones, the aggregation strategy of these parameters should be taken into account in any real retrieval scheme.

2) Errors on VWC: Since VWC was already pointed out as the main responsible of soil moisture errors [13], it is relevant to study which are the maximum error tolerable in this parameter in order to keep soil moisture error below a give value. To this end, error was added to high resolution ancillary parameter VWC before aggregation. In order to simulate both a systematic bias and variance in the VWC layer, errors were added as Gaussian noise $\mathcal{N}(0, \sigma^2)$ with higher standard deviation for areas with denser vegetation and a bias to account for nonlinearity between VWC and its satellite-derived proxy (i.e. NDVI, NDWI). Coarse resolution noisy VWC is then used in the soil moisture retrieval and the synthetic product performance is assessed. Results are summarized in Table II.

As expected, linear average of VWC exhibits strong sensitivity to biases on high resolution VWC. On the other hand, the performance of alternative aggregation method remains moderately constant when bias on VWC is added. Furthermore, for high bias cases (more than 25%), applying the alternative aggregation rule yields high accuracy on soil moisture retrieval in comparison with linear averaging. Both aggregation methods exhibits low sensitivity to Gaussian noise on high resolution VWC. This results is expected since random error (i.e. non-bias based) added was spatially independent in neighboring 1-km pixels. As a result, it can be effectively eliminated by spatial averaging. In summary, although accuracy decreases

when VWC error increases (both bias and variance), the retrieval model proves to be quite robust even when using low quality VWC data.

C. Composite

Results for the different implemented composites are shown in Fig. 3: nearest neighbor 3(a), weighing function 3(c) and local polynomial fitting 3(d). Since only ascending passes were considered in the simulation, composed soil moisture does not precisely represent the Level 3 processing (in fact the interpolation methods (1) and (2) led to some 'holes' in the soil moisture imagery). Nevertheless, several conclusions can still be extracted from the analysis. Interpolations (1) and (2) display the most similar results. However, nearest neighbor composite is more sensitive to noise on radiometer observations. Moreover, with this configuration, local polynomial fitting displays the lowest accuracy. However, further analysis should be carried out to reach the optimal bandwidth for the local polynomial compound and improve the estimation.

IV. Discussion & Conclusions

Using an OSSE for Aquarius, this study evaluated the accuracy of retrieving soil moisture from radiometer observations and the potential impact of different error sources over the final product. Product performance depends on interpretation of OSSEs results and error analysis, and different error metrics, as well as different objectives on the characteristics of the obtained imagery, will lead to different soil moisture maps. These latter should agree with users expectations.

After evaluating error metrics (correlation and RMSE), it has been showed that the single channel algorithm for retrieving soil moisture from brightness temperature observations displays high sensitivity to optical depth and vegetation water content aggregation technique [13]. Moreover, results exhibited a bias on highly vegetated areas for synthetic soil moisture retrieved from passive microwaves when linear averaging is used to aggregate VWC. Aggregation of vegetation water content impact is stronger at denser vegetation.

OSSE simulations were also used to evaluate and compare three different composing methods to obtain L3 product imagery. Results suggest that choosing an optimal soil moisture composite has a lesser impact of retrieval accuracy than improvement that can be achieved by implementing proper ancillary parameter aggregation methods.

Finally, both parameter uncertainty and instrumental errors were considered. Despite the low errors considered in the auxillary parameter, the retrieval was found to be more sensitive to ancillary parameter errors than to added footprint-scale noise over observations. Moreover, using OSSE outputs, both systematic and random errors in VWC data were studied for two different aggregation techniques (average and Zhan [14]). For large values of VWC, an overestimation of soil moisture is observed when averaging to degrade VWC. Regarding vegetation effects, an overestimation in soil moisture is related to an overestimation of VWC. Indeed, for a given value of measured Tb_H, the retrieval model will assign a higher soil moisture value to the most heavily vegetated areas. Therefore, the overestimation in soil moisture observed when averaging should be related to an overall overestimation of VWC for the areas characterized with large VWC values ($> 2\,Kg/m^2$). This was observed by Zhan [14], who proposed his own aggregation technique in order to solve this issue.

From previous studies [13] and the results of this paper, we established that, at first order, VWC is the parameter that controls estimated soil moisture error. Therefore, its absolute error and aggregation strategy should be comprehensively studied. In this paper, two sources of VWC error were studied: a zero mean Gaussian noise and a systematic bias (Table II). As expected, an increase in VWC errors degrades soil moisture estimation. Linear aggregation scheme is sensitive to biases on VWC. As already noted, Zhan aggregation errors remain more constant when bias on VWC is added. In general, although accuracy decreases when VWC error increases, the retrieval model presents a robust estimation even for large errors on VWC. Nevertheless, based on these simulations, maximum values for VWC errors (bias and std) can be defined. As a conservative estimation, for the dataset and configuration using in this OSSE, $VWC_{biasmax} \lesssim 12\%$.

It is interesting to contrast these values with the values available in the literature. VWC data used for passive microwave soil moisture retrieval is generally estimated using one or a combination of these remote sensing proxies: NDVI [18], NDWI [19] and microwave polarization indexes [20]. All these methods are landcover-dependent (i.e. the equations that relate the proxy value to VWC depends on assumptions about landcover). Nevertheless, not all this VWC estimation strategies are well validated, and only a few presents error estimations. As an example, [21] informs an RMS error $\sim 0.6\,kg/m^2$ for the estimation of VWC from NDWI (for corn and soybean), which accounts for $\sim 10\%$ of the observed VWC range for these crops. Therefore, these errors seem to be acceptable to use this estimated VWC as an input in a soil moisture retrieval scheme. Nevertheless, the same work informs on plots which present strong discrepancies with

the proposed VWC-NDVI model, and even nonlinear relationships between NDVI and VWC, which could lead to bias in linear interpolations, are reported [22]. Finally, this kind of exhaustive analysis is not present for all the landcovers, and therefore its is difficult to asses if current VWC estimations strategies are good enough to be used as an input in Aquarius soil moisture retrieval scheme.

ACKNOWLEDGMENT

This work was funded by the Agencia Nacional de Promoción Científica y Tecnológica (ANPCyT) (PICT 1203) and MinCyT-CONAE-CONICET project 12.

REFERENCES

[1] W. T. Crow, M. Drusch, and E. F. Wood, "An observation system simulation experiment for the impact of land surface heterogeneity on amsr-e soil moisture retrieval," *Geoscience and Remote Sensing, IEEE Transactions on*, vol. 39, pp. 1622 – 1631, Aug. 2001.

[2] W.T. Crow, S.T.K. Chan, D. Entekhabi, P.R. Houser, A.Y. Hsu, T.J. Jackson, E.G. Njoku, P.E. O'Neill, Jiancheng Shi, and Xiwu Zhan, "An observing system simulation experiment for hydros radiometer-only soil moisture products," *Geoscience and Remote Sensing, IEEE Transactions on*, vol. 43, no. 6, pp. 1289–1303, Jun. 2005.

[3] D.M. Le Vine, E.P. Dinnat, S. Abraham, P. de Matthaeis, and F.J. Wentz, "The aquarius simulator and cold-sky calibration," *Geoscience and Remote Sensing, IEEE Transactions on*, vol. 49, no. 9, pp. 3198 –3210, Sept. 2011.

[4] A. G. Konings, D. Entekhabi, S. T. K. Chan, and E. G. Njoku, "Effect of radiative transfer uncertainty on l-band radiometric soil moisture retrieval," *Geoscience and Remote Sensing, IEEE Transactions on*, vol. 49, no. 7, pp. 2686 – 2698, Jul. 2011.

[5] C. D. Peters-Lidard, M. S. Zion, , and E. F. Wood, "A soil-vegetation-atmosphere transfer scheme for modeling spatially variable water and energy balance processes," *J. Geophys. Res.*, vol. 102, pp. 4303–4324, Feb. 1997.

[6] T. J. Jackson and T. J. Schmugge, "Vegetation effects on the microwave emmision of soil," *Remote Sensing of Environment*, vol. 36, pp. 203 – 212, 1991.

[7] M.C. Dobson, F. T. Ulaby, M. T. Hallikainen, and M. A. El-Rayes, "Microwave dielectric behavior of wet soil-part ii: Dielectric mixing models," *Geoscience and Remote Sensing, IEEE Transactions on*, vol. GE-23, pp. 35 – 46, Jan. 1985.

[8] D. M. Le Vine, G. S. E. Lagerloef, S. Yueh, F. Pellerano, E. Dinnat, and F. Wentz, "Aquarius mission technical overview," *Geoscience and Remote Sensing Symposium, 2006. IGARSS 2006. IEEE International Conference on*, pp. 1678 – 1680, Jul. 2006.

[9] A. S. Limaye, W. L. Crosson, and C. A. Laymon, "Estimating accuracy in optimal deconvolution of synthetic amsr-e observations," *Remote Sensing of Environment*, vol. 100, no. 1, pp. 133–142, 2006.

[10] Yi Chao, "L2a aquarius science requirements," Tech. Rep., Jet Propulsion Laboratory, Jul. 2008.

[11] G. Foti and C. Finch, "Aquarius user guide," Tech. Rep., Jet Propulsion Laboratory, 2011.

[12] T. J. Jackson, "Measuring surface soil moisture using passive microwave remote sensing," *Hydrological Processes*, pp. 139–152, 1993.

[13] C.A. Bruscantini, F.M. Grings, P. Perna, H. Karszenbaum, W.T. Crow, and J.C.A. Jacobo, "An observing system simulation experiment (osse) for the aquarius/sac-d soil moisture product," in *Microwave Radiometry and Remote Sensing of the Environment (MicroRad), 2012 12th Specialist Meeting on*, Mar. 2012, pp. 1 –4.

[14] Xiwu Zhan, W.T. Crow, T.J. Jackson, and P.E. O'Neill, "Improving spaceborne radiometer soil moisture retrievals with alternative aggregation rules for ancillary parameters in highly heterogeneous vegetated areas," *Geoscience and Remote Sensing Letters, IEEE*, vol. 5, no. 2, pp. 261–265, Apr. 2008.

[15] J. M. Lilly and G. S. E. Lagerloef, "Aquarius level 3 processing algorithm theoretical basis document, part ii. implementation," Feb. 2009.

[16] E.P. Dinnat, D.M. Le Vine, S. Abraham, P. de Matthaeis, and C. Utku, "Comparison of aquarius measurements and radiative transfer models at l-band," in *Microwave Radiometry and Remote Sensing of the Environment (MicroRad), 2012 12th Specialist Meeting on*, Mar. 2012, pp. 1 –4.

[17] Christopher S. Ruf and Haiping Zhang, "Performance evaluation of single and multichannel microwave radiometers for soil moisture retrieval," *Remote Sensing of Environment*, vol. 75, no. 1, pp. 86 – 99, Jan. 2001.

[18] T. J. Jackson, D. M. Le Vine, A. Y. Oldak, P. J. Starks, C. T. Swift, J. D. Isham, and M. Haken, "Soil moisture mapping at regional scales using microwave radiometry: the southern great plains hydrology experiment," *Geoscience and Remote Sensing, IEEE Transactions on*, vol. 37, pp. 2136 – 2151, 1999.

[19] D. Chen, T. J. Jackson, F. Li, M. H. Cosh, C. Walthall, and M. Anderson, "Estimation of vegetation water content for corn and soybeans with a normalized difference water index (ndwi) using landsat thematic mapper data," *Geoscience and Remote Sensing Symposium, 2003. IGARSS '03. Proceedings. 2003 IEEE International*, vol. 4, pp. 2853 – 2856, 2003.

[20] T. Jing, S. Jiancheng, T. J. Jackson, D. Jinyang, R. Bindlish, and Z. Lixin, "Monitoring vegetation water content using microwave vegetation indices," *Geoscience and Remote Sensing Symposium, 2008. IGARSS 2008. IEEE International*, vol. 1, pp. I–197 – I–200, 2008.

[21] D. Chen, J. Huang, and T. J. Jackson, "Vegetation water content estimation for corn and soybeans using spectral indices derived from modis near- and short-wave infrared bands," *Remote Sensing of Environment*, vol. 98, no. 2–3, pp. 225 – 236, 2005.

[22] T. J. Jackson, D. Chen, M. Cosh, F. Li, M. Anderson, C. Walthall, P. Doriaswamy, and E. Ray Hunt, "Vegetation water content mapping using landsat data derived normalized difference water index for corn and soybeans," *Remote Sensing of Environment*, vol. 92, no. 4, pp. 475 – 482, 2004.

Cintia A. Bruscantini is an electronic engineer currently pursuing the engineering Ph.D. degree in observing systems simulations at the Instituto de Astronomía y Física del Espacio (IAFE), Buenos Aires, Argentina. She has been working on developing an Observing System Simulation Experiment (OSSE) for the Aquarius soil moisture product. She is also collaborating with the National Commission on Space Activities (CONAE) of Argentina for the calibration of the microwave radiometer (MWR) on board the Aquarius/SAC-D.

Francisco Grings received the Ph.D. degree in 2008. He is a physicist and a junior research member of Consejo Nacional de Investigaciones Científicas y Técnicas (CONICET) working at Instituto de Astronomía y Física del Espacio (IAFE), Buenos Aires, Argentina. He is responsible for remote sensing modeling within IAFE's remote sensing group. He is leading the Observing System Simulation Experiment (OSSE) project at IAFE.

Pablo Perna is a student in computer science finishing his career at the University of Buenos Aires. He is a consultant for Instituto de Astronomía y Física del Espacio (IAFE), Buenos Aires, Argentina, and responsible for computer simulations and data acquisition algorithms.

Martin Maas is currently pursuing the Licenciatura degree in Applied Mathematics, at the University of Buenos Aires. He works in numerical electromagnetics and statistical modelling in microwave remote sensing, at IAFE (Instituto de Astronomía y Físca del Espacio).

Haydee Karszenbaum is a physicist and research member of Consejo Nacional de Investigaciones Científicas y Técnicas (CONICET), a remote sensing specialist, and Director of the Remote Sensing Group at the Instituto de Astronomía y Física del Espacio (IAFE), Buenos Aires, Argentina. Since 1983, she has worked in remote sensing, and since 1997, she has been dedicated to microwave remote sensing. She is currently the PI of national projects and of Space Agencies AO projects. She is also coordinating a technology transfer project related to applications and quality analysis of the future Argentine SAOCOM SAR mission products.

Wade T. Crow (M'03) received the Ph.D. degree from Princeton University, Princeton, NJ, in 2001. He is currently a Research Scientist with the Hydrology and Remote Sensing Laboratory, Agricultural Research Service, U.S. Department of Agriculture, Beltsville, MD. His research involves the application of land surface modeling and remote sensing technology to hydrology and agriculture.

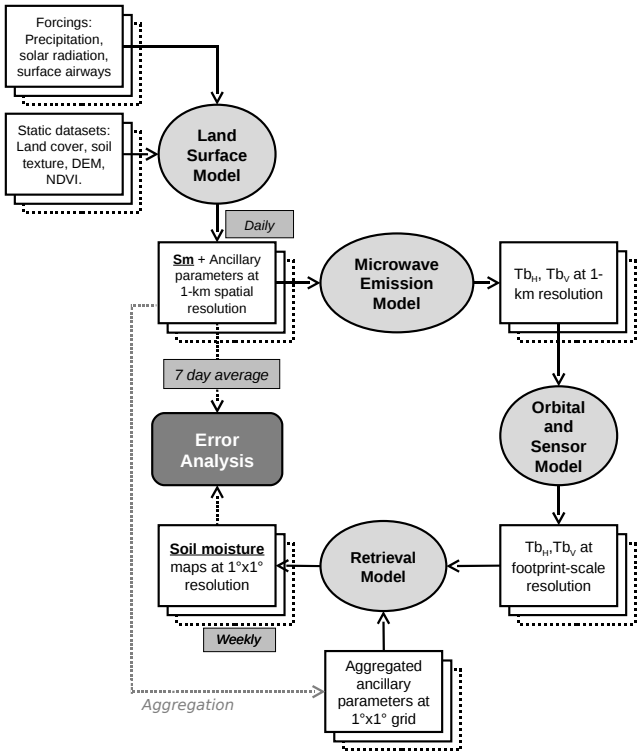

Fig. 1. OSSE Block Diagram

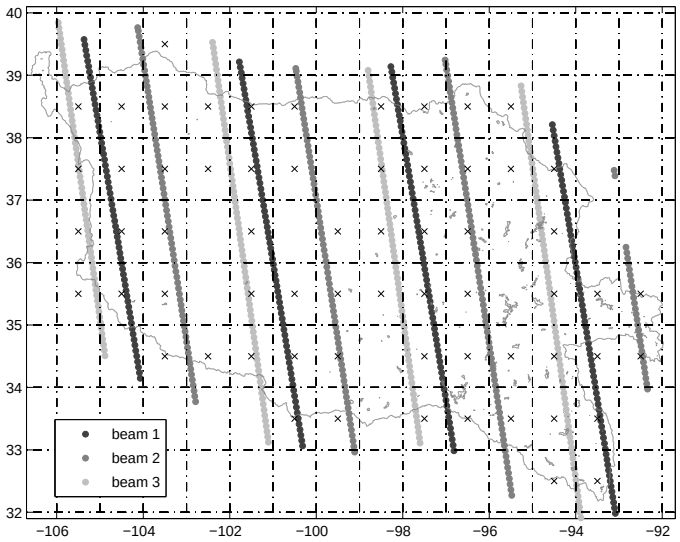

Fig. 2. Weekly composite at 1° grid of soil moisture product derived from the three Aquarius beams. Composite location is marked with 'x' and soil moisture product before gridding is marked with filled 'o'

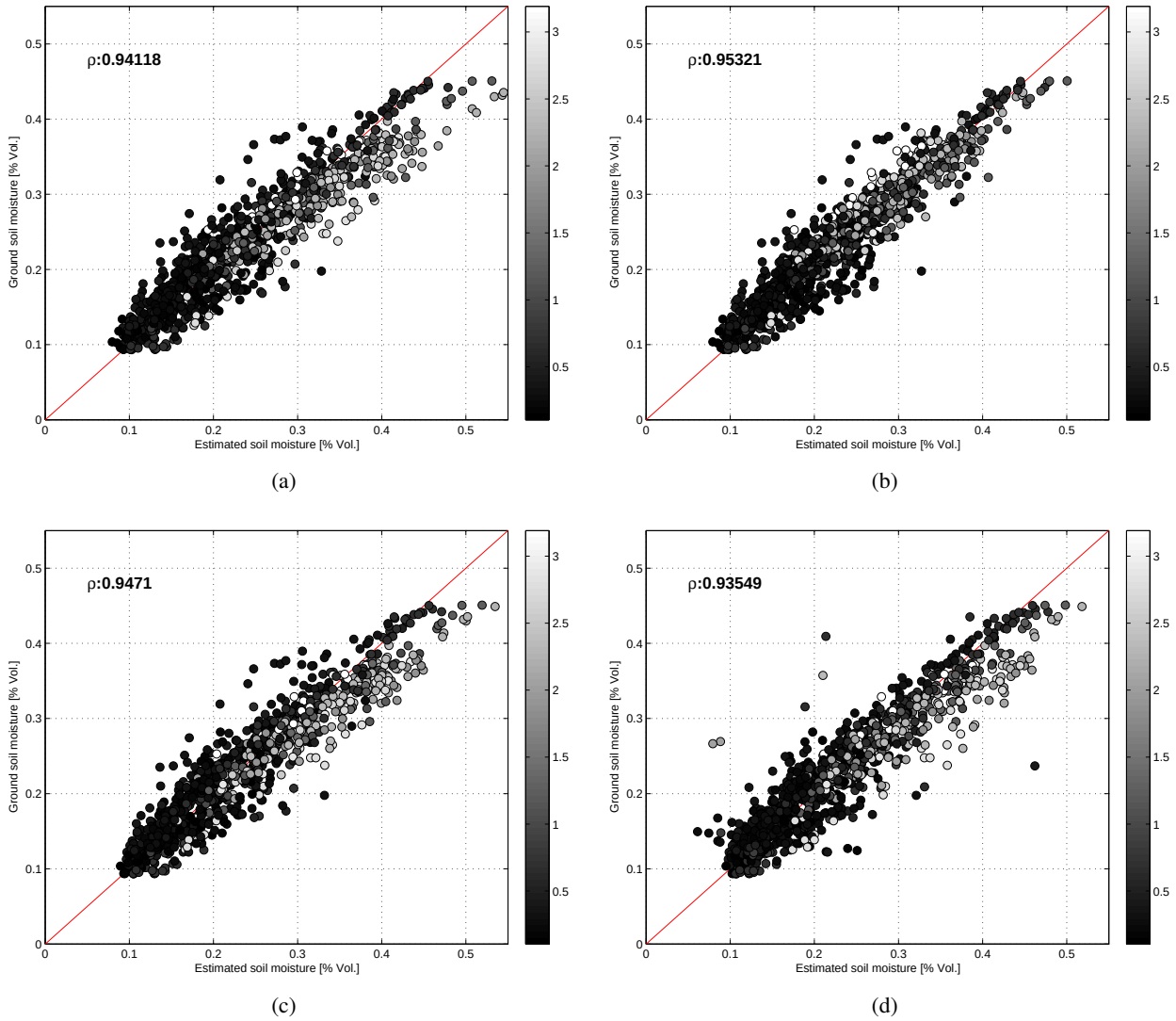

Fig. 3. Ground soil moisture vs. estimated soil moisture from horizontal polarization channel for different VWC aggregation methods and soil moisture composites: averaged VWC and nearest neighbour composite (a); aggregated VWC and nearest neighbour composite (b); averaged VWC and weighing function (c); averaged VWC and local second order polynomial fitting (d). Color axes correspond to VWC $[kg/m^2]$ values.

TABLE I
ERROR METRICS

		NN				**WF**				**LP**			
		Tb_h		Tb_v		Tb_h		Tb_v		Tb_h		Tb_v	
		ρ	rmse	ρ	rmse	ρ	rmse	ρ	rmse	ρ	rmse	ρ	rmse
AV	nn	0.941	0.034	0.952	0.030	0.947	0.031	0.955	0.029	0.935	0.034	0.951	0.030
	i	0.940	0.034	0.952	0.030	0.947	0.031	0.955	0.029	0.935	0.035	0.948	0.031
	i+p	0.937	0.036	0.950	0.031	0.946	0.032	0.955	0.029	0.933	0.035	0.943	0.032
AGG	nn	0.953	0.028	0.957	0.027	0.957	0.027	0.959	0.026	0.948	0.029	0.952	0.028
	i	0.953	0.028	0.957	0.027	0.957	0.027	0.959	0.026	0.939	0.032	0.950	0.029
	i+p	0.951	0.028	0.956	0.027	0.956	0.027	0.959	0.026	0.931	0.033	0.941	0.031

TABLE II
ERRORS ON VWC

VWC Agg.		**No Error**	**5% bias +10% σ**	**5% bias +15% σ**	**5% bias +25% σ**	**8% bias +15% σ**	**8% bias +25% σ**	**12% bias +15% σ**	**25% bias +25% σ**
AV	ρ_h	0.941	0.933	0.933	0.933	0.929	0.929	0.918	0.878
	$RMSE_h$	0.034	0.040	0.040	0.040	0.044	0.043	0.052	0.083
	ρ_v	0.952	0.950	0.950	0.950	0.949	0.949	0.946	0.937
	$RMSE_v$	0.030	0.033	0.033	0.033	0.034	0.034	0.037	0.048
AGG	ρ_h	0.953	0.925	0.925	0.924	0.924	0.923	0.920	0.911
	$RMSE_h$	0.028	0.035	0.036	0.036	0.036	0.037	0.039	0.048
	ρ_v	0.957	0.927	0.926	0.926	0.926	0.926	0.924	0.921
	$RMSE_v$	0.027	0.036	0.036	0.036	0.036	0.037	0.038	0.042

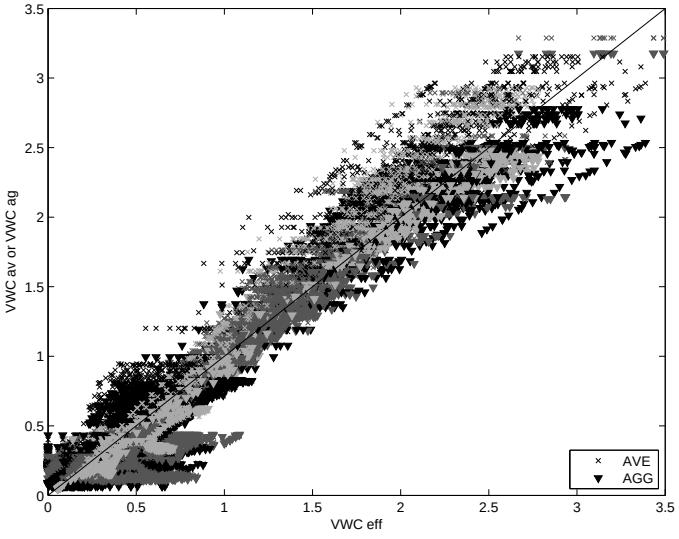

Fig. 4. Comparison between averaged (AVE) and aggregated (AGG) VWC values and corresponding effective VWC values (EFF).Black color corresponds to Aquarius inner footprint incidence angle, gray to the middle one and light gray to the outter one.